The American Journal of Human Genetics, Volume *103*

Supplemental Data

Bi-allelic *TMEM94* Truncating Variants Are Associated with Neurodevelopmental Delay, Congenital Heart Defects, and Distinct Facial Dysmorphism

Joshi Stephen, Sateesh Maddirevula, Sheela Nampoothiri, John D. Burke, Matthew Herzog, Anju Shukla, Katharina Steindl, Ascia Eskin, Siddaramappa J. Patil, Pascal Joset, Hane Lee, Lisa. J. Garrett, Tadafumi Yokoyama, Nicholas Balanda, Steven P. Bodine, Nathanial J. Tolman, Patricia M. Zerfas, Allison Zheng, Georgia Ramantani, Katta M. Girisha, Cecilia Rivas, Pujar V. Suresh, Abdel Elkahloun, Hessa S. Alsaif, Salma M. Wakil, Laila Mahmoud, Rehab Ali, Michaela Prochazkova, Undiagnosed Diseases Network members, Ashok B. Kulkarni, Tawfeg Ben-Omran, Dilek Colak, H. Douglas Morris, Anita Rauch, Julian A. Martinez-Agosto, Stanley F. Nelson, Fowzan S. Alkuraya, William A. Gahl, and May Christine V. Malicdan

Supplemental Data

Supplemental figures and legends

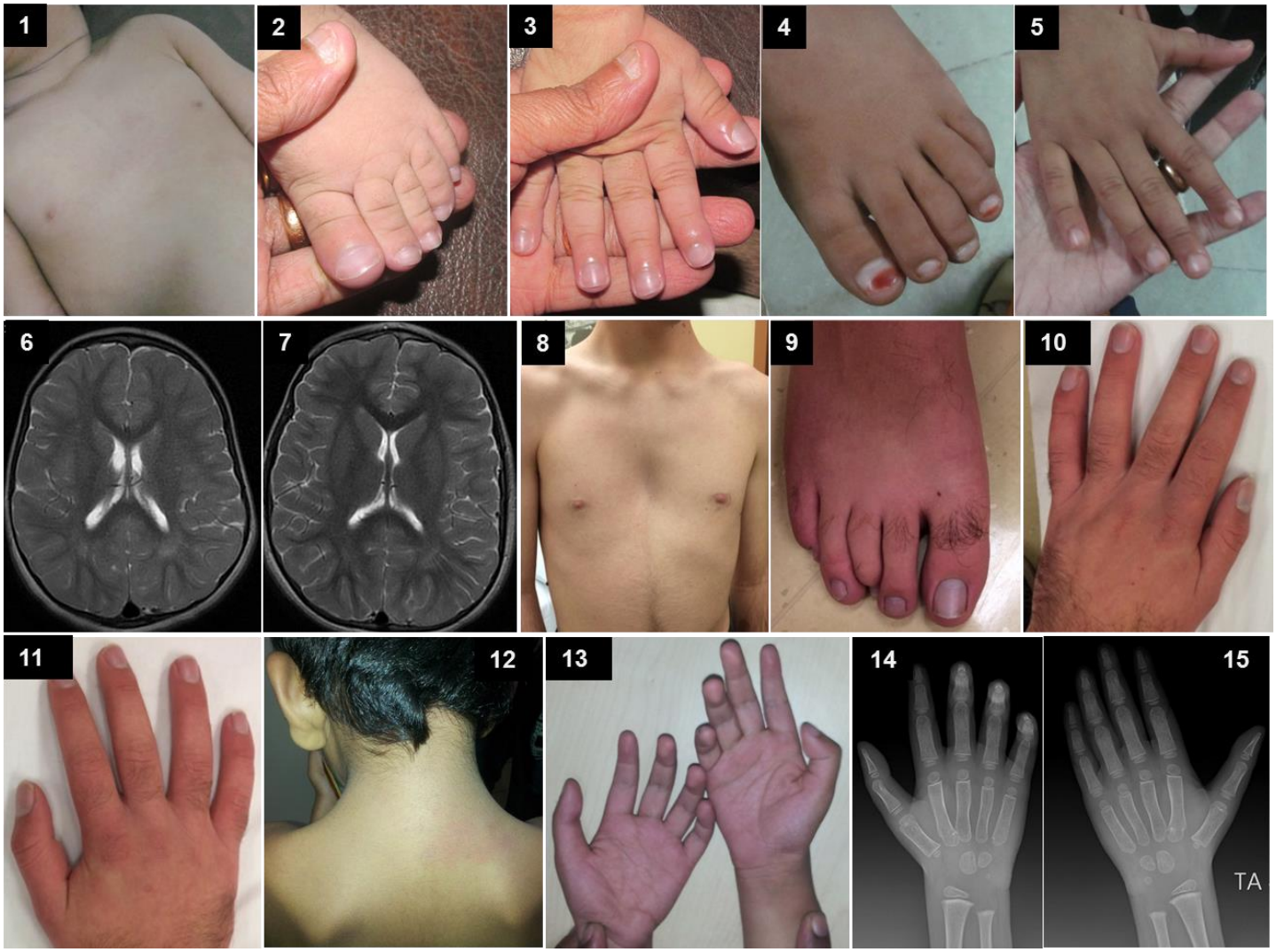

Figure S1: Additional clinical photographs of the families

(1-7) Photograph of proband (1-II.4 in Figure 1A) showing wide spaced nipples (1), normal toes and fingers (2 and 3; cyanosis and clubbing due to heart disease) and his affected elder sister (1-II.1 in Figure 1A) presented with long fingers and toes (4 and 5). MRI findings of both the affected members in family 1 were normal (6 is of 1-II.4 and 7 is of 1-II.1). (8-11) Photograph of the proband in family 3 showing pectus excavatum (8), bilateral overlapping of the 3rd toe by the 2nd and 4th toes (9) and arachnodactyly of the fingers (10, 11). (12-15) Photograph of the proband in family 4 showing webbed neck (12), slender fingers and fetal finger pads (13) and X-ray showing no significant skeletal defects (14, 15).

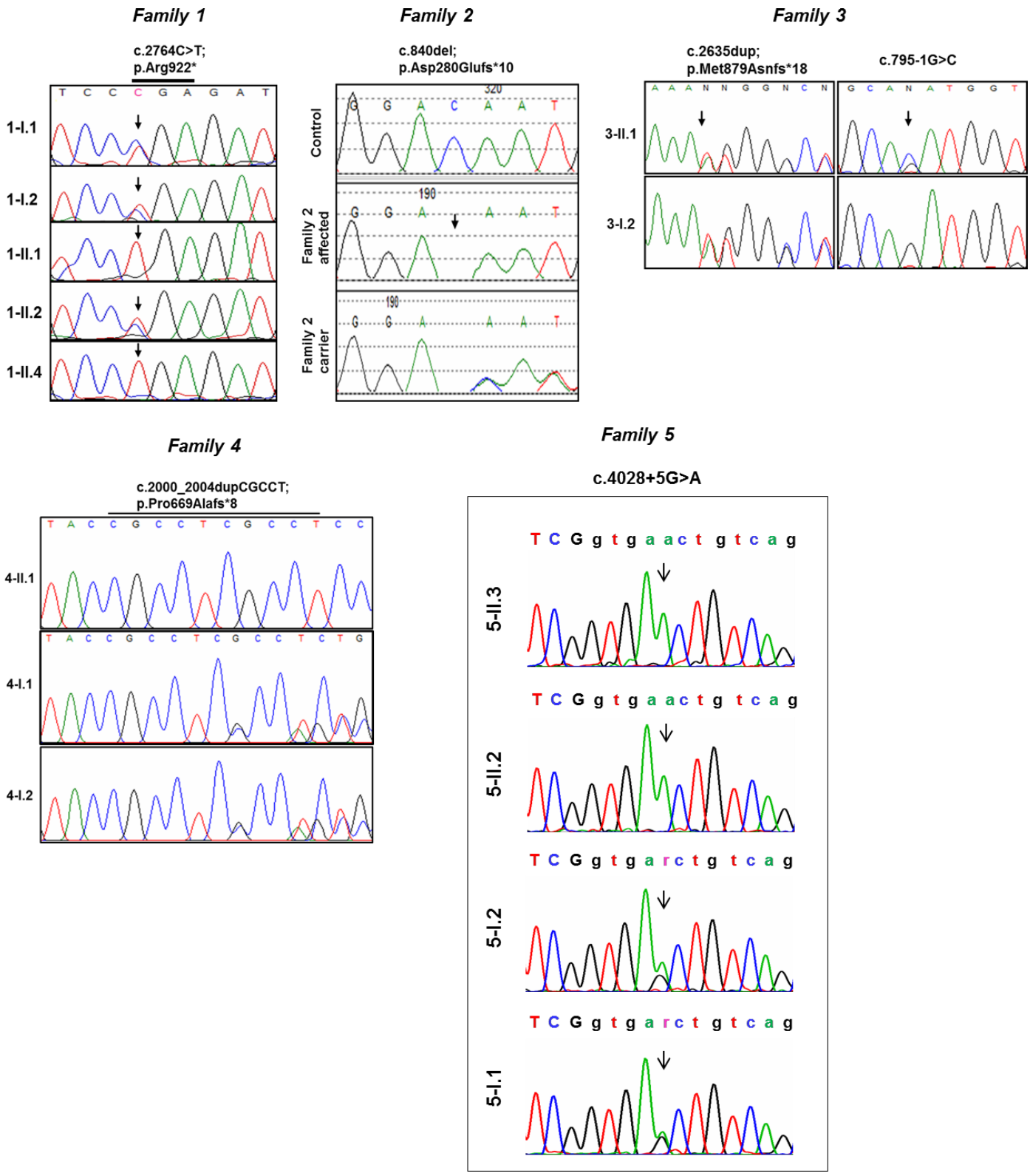

Figure S2: Sanger validation of *TMEM94* variants in genomic DNA level

Sanger confirmation and segregation of variants in in each family are shown. Family number in respect to corresponding pedigree number in figure 1A and variants in each family are also mentioned.

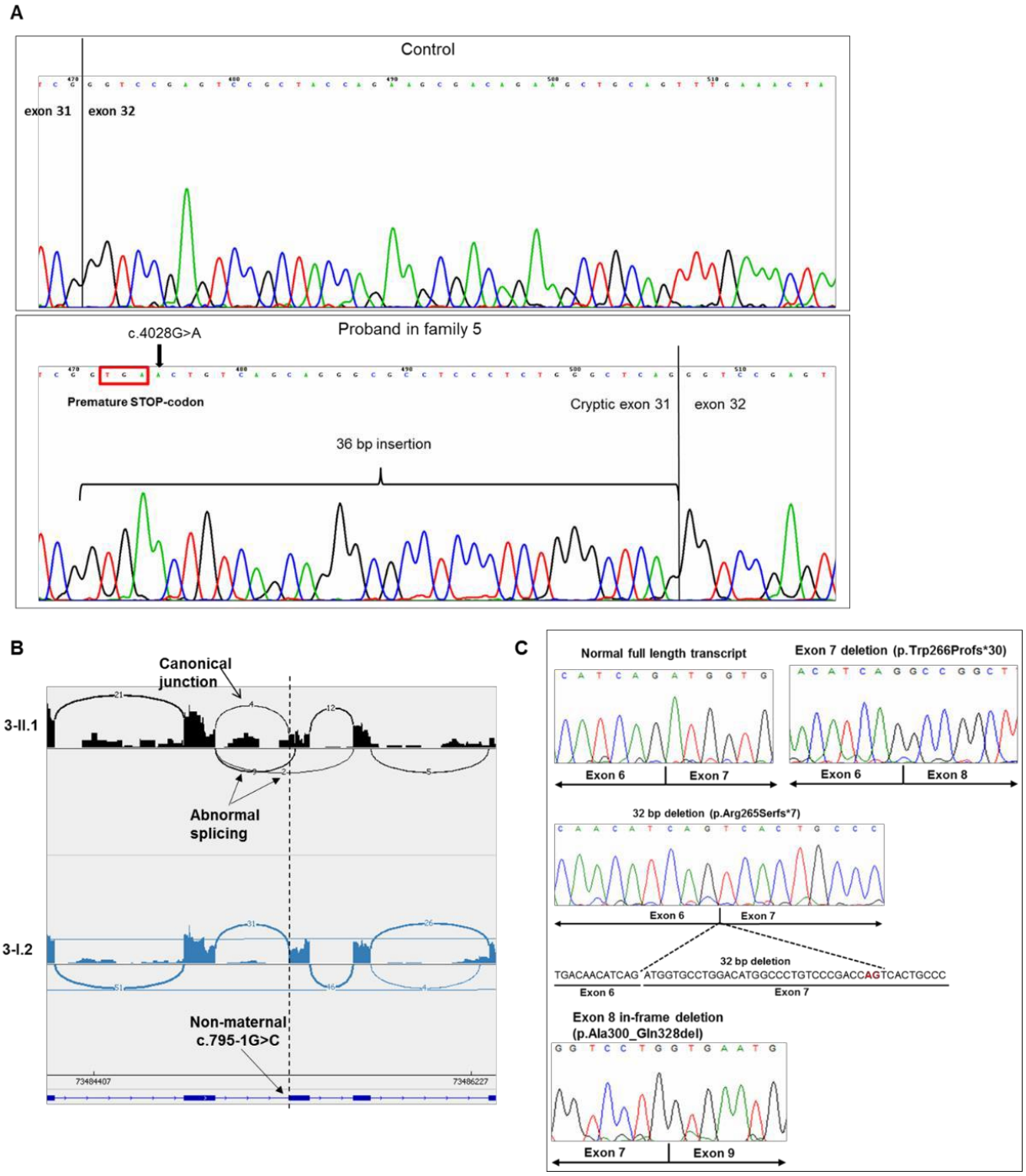

Figure S3: Splice site analysis on cDNA derived from the probands of family 3 and 5

(**A**) cDNA sequencing of primers flanking c.4028+5G>A variant in family 5 revealed an abnormal insertion due to an activation of a cryptic donor site 36 bp downstream within the intron compared to control. The aberrant transcript is predicted to result in a premature termination codon (red box) (**B**) Sashimi plot showing the splice alteration in the proband (3-II.1) as a result of a splice acceptor variant c.795-1G>C. Two different splice alterations were observed: 2 reads supporting exon skipping and 9 reads supporting a cryptic splice site created within an exon. Mother (3-I.2) did not carry the variant and shows normal canonical splice junctions (**C**) Multiple mutant transcripts were identified in the proband of family 3 (3-II.1) due to splice defect (shown in main figure 2C). The PCR products were subcloned in to TOPO vector and sequenced to confirm the mutant cDNA sequence. Sanger sequencing chromatograms showing the full-length transcript, exon 7 and exon 8 skipping and the 32bp deletion due to the activation of a cryptic acceptor site in the exonic region (of exon 7) are shown.

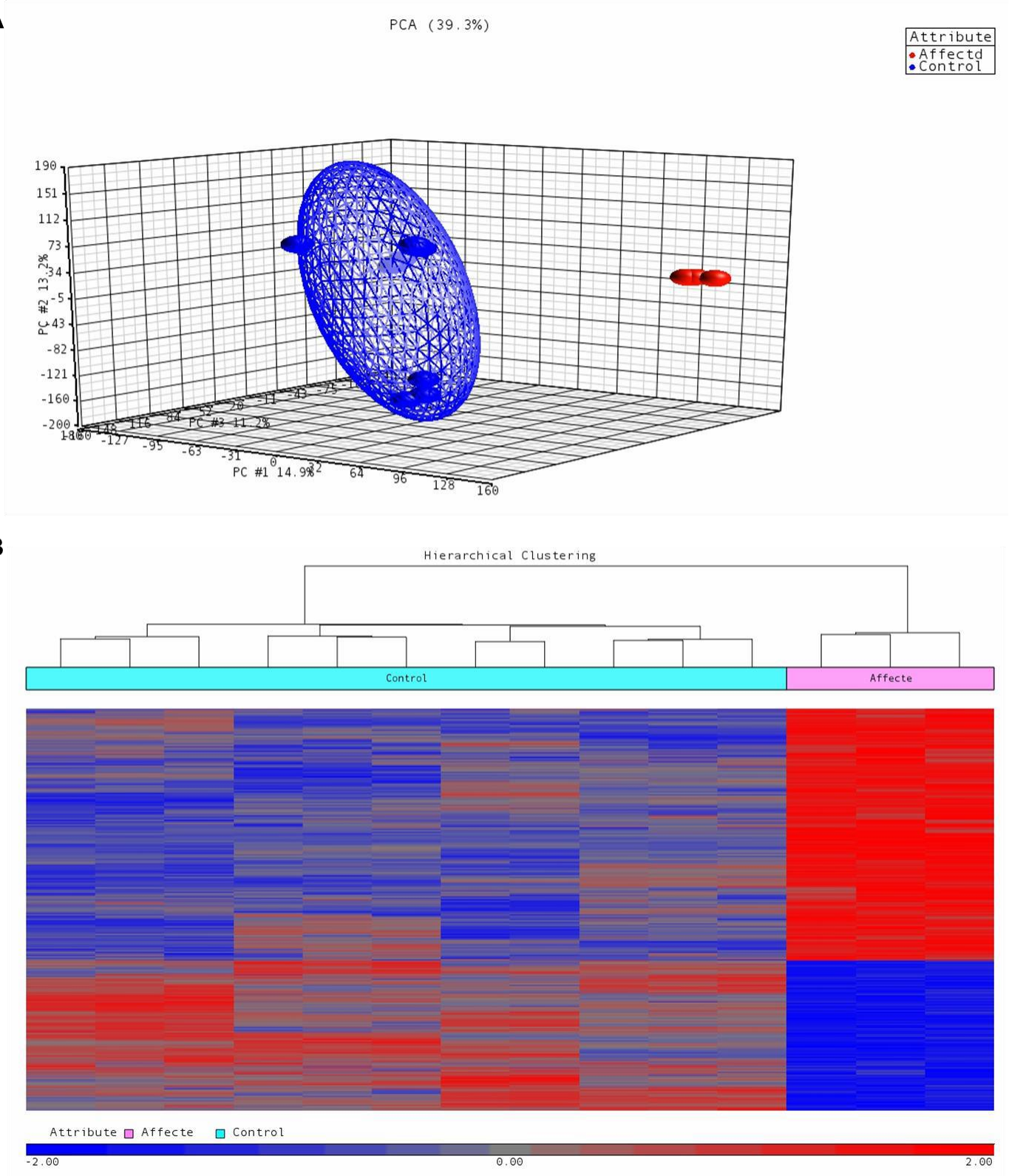

Figure S4: Global gene expression profiling using microarray

(**A**) Principal component analysis (PCA) and (**B**) Heatmap of genes that are significantly dysregulated in *TMEM94* deficient individual compared to controls. The expression level of each gene across the samples is scaled to [-2,2] interval.

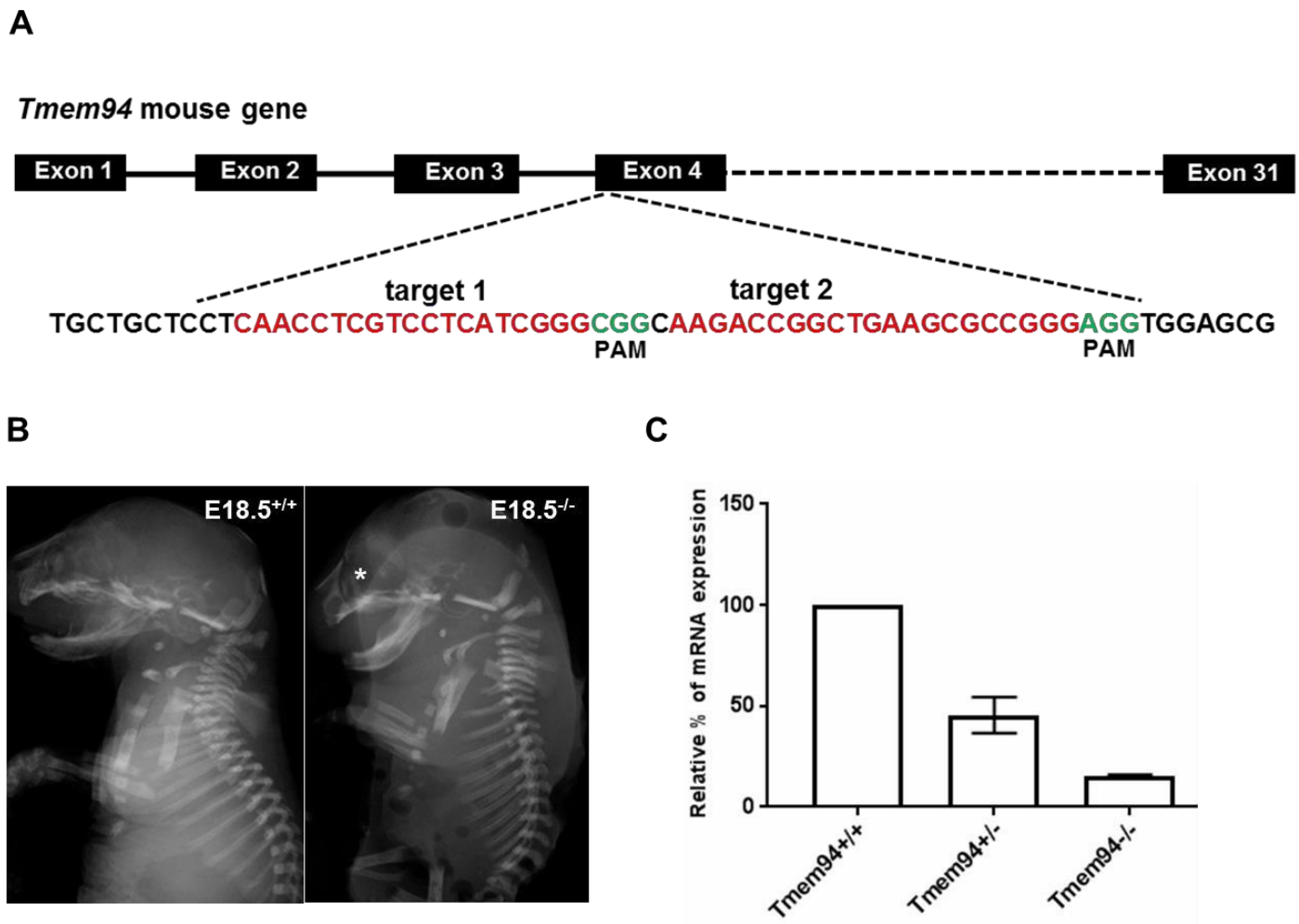

Figure S5: *Tmem94*$^{-/-}$ mice additional data and phenotype

(A) Schematic diagram representing *Tmem94* mouse gene and the two genomic targets (in exon 4) for CRISPR/Cas9 editing. Red highlighted areas are the two genomic targets in exon 4 and the nucleotides highlighted in green are PAM sequences (NGG), one for each target. The Cas9 is expected to cut few nucleotides upstream to the PAM sequence of each target (**B**) X-ray radiographs of wild type (left) and mutant (right) at E18.5 days showing reduced nasal bones in the mutant (asterisk) suggesting craniofacial abnormalities. (**C**) Relative quantification of mRNA level in *Tmem94* mutant embryos. Results were normalized to the expression of the housekeeping gene, *Polr2a*. Error bar represents standard deviation of mean expression in biological replicates.

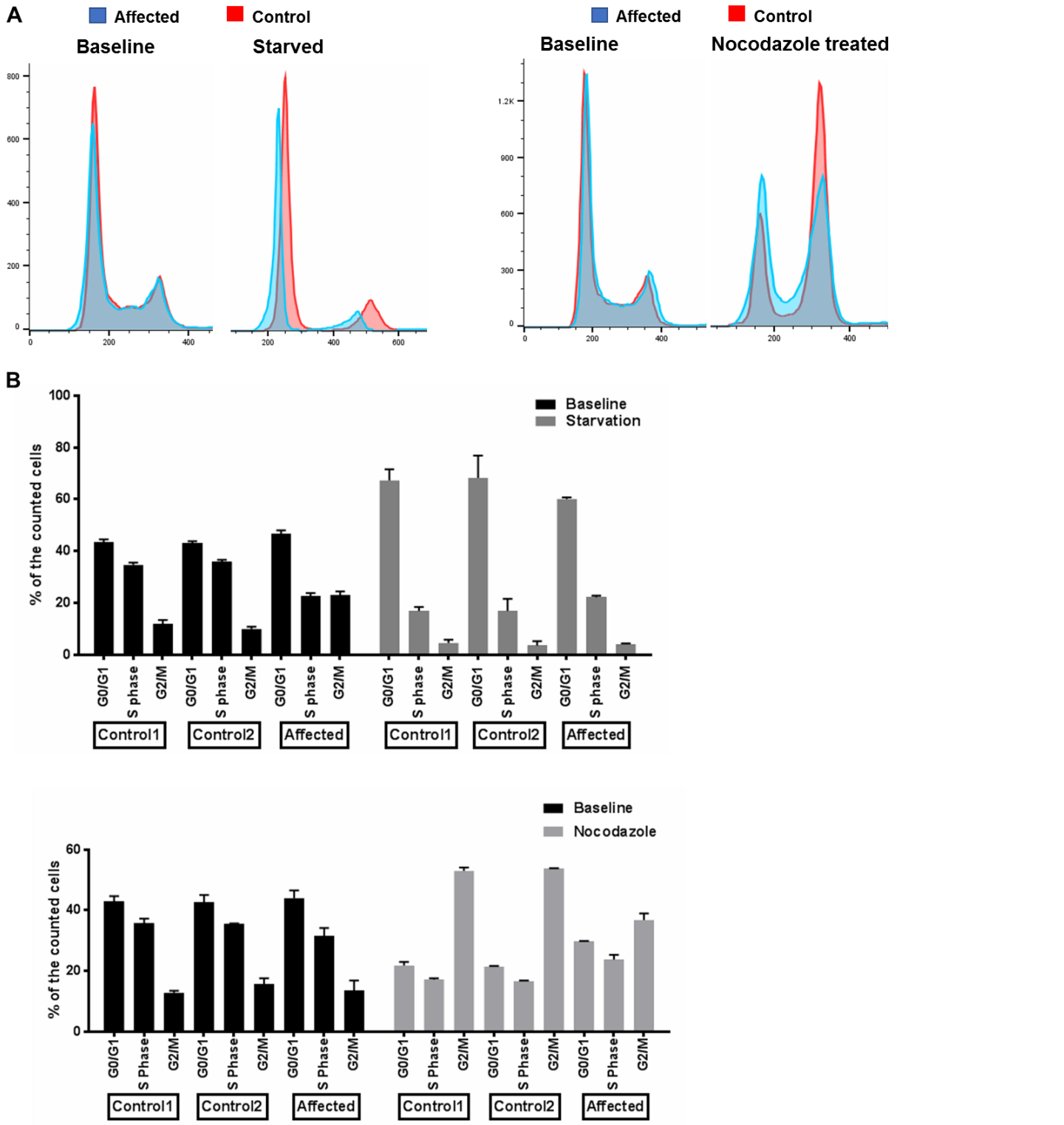

Figure S6: Flow cytometry measurement of DNA content of cells at different stages of cell cycle

(**A**) Representative cell cycle profile of control and proband derived fibroblasts (Blue: affected, Red: Controls) showed elevated percentage G0/G1 cells and lower percentage of the cells in G2/M phase in normal baseline condition. Upon starvation, G0/G1 were further elevated and G2/M phase cells were reduced in both control and affected (left panel). Overnight nocodazole treatment that arrests cells at G2/M phase of cell cycle, showed reduced percentage of G2/M phase cells in the affected, compared to the controls (right panel). (**B**) Graph showing the quantification of the experiment performed in starvation (Upper panel) and nocodazole treatment (lower panel). Experiments were done in triplicates and the error bar represents standard deviation of means.

Supplemental tables

Purpose	Primer sequence
Targeting oligos	Target 1: 5'-CCTCAACCTCGTCCTCATCGGGC-3' Target 2: 5'-GCAAGACCGGCTGAAGCGCCGGG-3'
For in-vitro transcription	Oligo 1 5'-*tttttaatacgactcactata*GGCCGATGAGGACGAGGTTGgttttagagctagaa-3' Oligo 2 5'-*tttttaatacgactcactata*GGAAGACCGGCTGAAGCGCCgttttagagctagaa-3' Low caps, Italics: T7 promoter region High caps: genomic target region Low caps, underlined: universal reverse primer binding region
	Universal reverse primer 5'-aaaagcaccgactcggtgccacttttcaagttgataacggactagccttattttaacttgctatttctagctctaaaac- 3' Low caps, underlined: Oligo annealing region
Mouse genotyping	Forward: 5'-GAGGTGGCCATAAGAAATAGGC-3' Reverse: 5'-TGGTGACCGTGGCTATCCTA-3'
Human cDNA splice analysis	Forward: 5'-GGGATCAAGGATGACGAGCA-3' Reverse: 5'-GAGGACTGGAAAGAGCAGGG-3'
M13 Primers for the sequencing of the clones	Forward: 5'-GTAAAACGACGGCCAG-3' Reverse: 5'-CAGGAAACAGCTATGAC-3'
Human qPCR	*TMEM94* Forward: 5'-CTGCGAGGGATCATTGACCA-3' Reverse: 5'-CTCTGTAGGCCCAGTGCAAG-3'
	POLR2A Forward: 5'-CATGTGCAGGAAACATGACA-3' Reverse: 5'-GCAGAAGAAGCAGACACAGC-3'
Mouse qPCR analysis	*Tmem94* Forward: 5'-GCGAGGAAGACCGTCCGA-3' Reverse: 5'-TGCTTCTCCCTCAGGTCCAT-3'
	Polr2a Forward: 5'-GCACCATCAAGAGAGTGCAG-3' Reverse: 5'-GTGGATCCATTAGTCCCCCA-3'

Table S1. **Primers used in this study**

DNA oligos/primers used guide RNA synthesis, genotyping, cDNA analysis and qPCR

Family	Chromosome	Homozygous stretch	Candidate genes in the homozygous area
Family 1	2	190,970,774 - 207,953,087	*NEMP2*
	4	91,295,654 - 122,902,899	None
	6	19,613,977 - 30,773,676	None
	9	4,093,145 - 11,256,115	None
	10	53,838,897 - 73,570,900	None
	15	22,559,617 - 35,528,037	None
	16	80,593,096 - 86,485,811	None
	17	65,148,725 - 78,360,332	*TRIM65*, ***TMEM94***
	18	70,471,959 - 73,808,200	None
	19	9,465,329 - 44,716,770	*SAMD4B*
	20	57,088,334 - 63,025,520	None
Family 2	1	29,190,140-39,500,180	*SERINC2*
	2	142,742,400-154,088,500	None
	4	156,893,000-161,004,600	None
	17	71,232,690-75,876,620	***TMEM94***
Family 4	1	753,541-4,592,116	None
	1	4,598,021-8,345,298	None
	1	8,356,170-14,864,580	None
	5	10,111,180-15,729,889	None
	6	68,452,823-77266188	None
	6	99,462,075-103,188,348	None
	7	53,998-5,214,016	None
	7	6,650,687-13,277,948	None
	8	55,402,535-63,461,952	None
	8	63,490,414-72,299,671	None
	11	204,228-4,460,348	*TRPM5*
	12	19,756,366-24,482,034	None
	12	47,492,686-62,969,704	None
	12	117,988,186-121,821,654	None
	12	121,847,135-124,891,294	None

	12	124,902,199-130,225,459	*TMEM132B*
	14	33,126,223-49,609,674	None
	14	52,640,208-57,040,997	None
	17	68,506,237-75,539,771	***TMEM94***
Family 5	1	27,543,522-34,206,979	None
	2	56,480,570-60,580,831	None
	6	117,392,770-121,904,036	None
	6	134,378,251-138,898,188	*IL20RA*
	7	130,915,278-134,242,036	None
	11	2,252208-6,324,678	None
	12	53,364,506-57,179,340	None
	16	30,444,444-35,220,544	None
	17	72,044,131-75,164,427	***TMEM94****, ITGB4*

Table S2. Regions of homozygosity

Homozygous regions segregating with the proband and affected siblings in consanguineous families

	Family 1	Family 2	Family 4	Family 5
Total number of variants	82,025	71,450	39,739	92,141
Homozygous variants	35,509	33,781	15,539	29,675
Exonic and splicing	9160	8,777	11,079	10,404
Allele frequency <0.01 in ExAC database	95	386	204	232
Number of variants with no healthy homozygote in ExAC database	34	297	95	225
Number of variants present in homozygous area	11	9	21	6
Number of variants segregate with the affected sibling and predicted to be pathogenic according to prediction tools	4	2	3	2

Table S3. **Filtering strategy of variants identified in the four consanguineous families (Family 1, 2, 4 and 5)**

Variant filtering and identification of segregated variants in the homozygous area

Total number of variants	5,101,964
Exonic and splicing	26,661
Missense + LoF variants	10,366
Allele frequency <0.01 in ExAC database	1,772
Number of variants with no healthy homozygote in ExAC database	1,477
Number of heterozygous variants that are greater than or equal to 2 for each gene	27 (10 genes)
Number of compound heterozygous variants (Father DNA sample was unavailable so the variants that are not inherited from the mother was assumed to be inherited from the father) + number of assumed *de novo* variants (heterozygous variants that are not inherited from the mother and not seen as heterozygous in ExAC database)	6

Table S4: Variant filtering strategy of family 3

Filtering strategy of the variants identified through whole genome sequencing in the affected individual of family 3

Family	**Genomic position**	**Gene**	**Variant**	**CADD score**	**Allele frequency in ExAC**	**SIFT**	**Mutation Taster**	**Polyphen -2**
Family 1	Chr2: 191383489A>C	*NEMP2*	c.491T>G p.Leu164Arg	16	Not present in ExAc and gnomAD	Deleterious	Disease causing	Probably damaging
	Chr17: 73887162G>A	*TRIM65*	c.1252C>T p.Arg418Trp	15	**0.0001726**	Deleterious	Disease causing	Probably damaging
	Chr17: 73491370C>T	***TMEM94***	**c.2764C>T, p.Arg922***	**43**	**0.0000086**	**NA**	**Damaging**	**NA**
	Chr19: 39867411G>A	*SAMD4B*	c.1084G>A, pVal362Ile	17	0.0000165	Tolerated	Disease causing	Probably damaging
Family 2	Chr1: 31906993T>C	*SERINC2*	c.1327T>C p.Tyr443His	28.8	NA	Deleterious	Disease causing	Probably damaging
	Chr17: 73485392del	***TMEM94***	**c.840del, p.Asp280Glufs*10**	**NA**	**NA**	**NA**	**NA**	**NA**
Family 3	**17:73485346**	***TMEM94*[b]**	**NM_001321148.1: c.795-1G>C**	**21**	**NA**	**NA**	**Damaging**	**NA**

	17:73490987	***TMEM94*[a]**	**NM_001321148.1: c.2635dupA; p.(Met879Asnfs*18)**	**NA**	**NA**	**NA**	**NA**	**NA**
	20:62194000	*HELZ2* [a] (MIM611265)	NM_001037335.2: c.6175C>T; NP_001032412.2:p.Arg2059Trp	5	0.00044681	Damaging	Tolerated	Benign
	20:62195413	*HELZ2* [b]	NM_001037335.2: c.4762G>C; NP_001032412.2:p.Gly1588Arg	0	0.00000992	Tolerated	Tolerated	Benign
	8:61774792	*CHD7* [b] (MIM 608892)	NM_017780.3:c.7868C>T; NP_060250.2:p.Pro2623Leu	33	NA	Damaging	Damaging	Probably Damaging
	1:7724106	*CAMTA1* [b] (MIM 611501)	NM_015215.2:c.1499G>C; NP_056030.1:p.Gly500Ala	19	NA	Damaging	Damaging	Probably Damaging
Family 4	Chr11: 2434775G>A	*TRPM5*	c.1934C>T: p.Thr645Met	24.6	0.000008736	Deleterious	Disease causing	Probably damaging
	Chr12: 126138252T>C	*TMEM132B*	c.769T>C: p.Trp257Arg	25.4	0.00001656	Deleterious	Disease causing	Probably damaging
	Chr17: 73489067_73489071dup	***TMEM94***	**c.2000_2004dup; p.Pro669Alafs*8**	**NA**	**NA**	**NA**	**NA**	**NA**
Family 5	Chr17: 73725516 C>T	*ITGB4*	c.737C>T: p.(Thr246Met)	**NA**	NA	Deleterious	Disease causing	Probably damaging
	Chr17: 73495168G>A	***TMEM94***	**c.4028+5G>A; p.?**	**NA**	**NA**	**NA**	**NA**	**NA**
Family 6	**Chr17: 7349392del**	***TMEM94***	**c.3497delA; p.Asn1166Thrfs*84**	**NA**	**NA**	**NA**	**NA**	**NA**
	Chr17: 78087081G>A	*GAA*	c.2105G>A; p.Arg702His	32	0.00005	Deleterious	Disease causing	Probably damaging

a, maternal; b, non-maternal; NA, not available

Table S5. Final list of variants in in all families

Final list of variants that are segregated with affected individuals of all 6 families. For family 1, 2, 4, 5 and 6 all the variants shown are homozygous and for family 3, all the variants listed are heterozygous. In family 1, all four variants were heterozygous in the unaffected sibling and parents (Figure 2A-II.2), and homozygous in both affected individuals (Figure 2A-II.1 and II.4). In family 2, the two variants (in *SERINC2* and *TMEM94*) were segregated with the affected status. Truncating variants in *TMEM94* is common in all families.

Gene	Log_2 Fold Change	*P*-adjusted value
Downregulted genes		
PTN	-5.431	0.036297
RNU5F-1	-1.799	0.046349
WWC1	-1.765	0.048065
HSPA7	-1.546	0.018122
ABCA10	-1.404	2.24E-08
FEZ1	-1.115	0.003138
TP73	-1.166	0.010215
SAT1	-1.098	0.000908
TMEM94	-0.932	3.72E-06
WSB2	-0.909	0.009543
PIGZ	-0.845	0.01331
DDIT4	-0.781	0.005472
LSM10	-0.527	0.009628
SNRPA	-0.53	0.0205
NPRL3	-0.278	0.049298
LSM14B	-0.259	0.034164
DCAF16	-0.245	0.021265
Upregulated genes		
CUL4A	0.264	0.027476
C5orf24	0.305	0.034925
ZNF525	0.456	0.005502
N4BP2	0.623	0.019307
HSPBAP1	0.651	0.027831
RBM3	0.655	0.001065
ARL14EP	0.772	0.000299
TP63	0.862	0.010919
ERMAP	0.907	0.000539
ADO	0.948	0.02027
ZNF239	0.911	0.046975
PCBD2	1.059	0.003243
DHRS3	1.514	0.021039
DAB2IP	2.376	0.000176
WFDC2	3.963	2.27E-07

Table S7. List of genes in the *TMEM94* interaction network identified in all the affected siblings in family 2

Detailed table displaying the fold change equal or greater than 1.5, with their corresponding *P*-adjusted values of genes identified in TMEM94 interaction network of dysregulated genes identified through RNA Sequencing (Benjamini-Hochberg correction for multiple comparisons). Interestingly, some of the genes identified have profound role in neurological function; *RBM3* (MIM 300027), which is associated with synapse regeneration[1] and shown to interact with TMEM94[2]; *PTN* (MIM 162095), a mitogenic protein involves in neurite outgrowth and embryogenesis[3], *TP73* (MIM 601990), which is thought to be involved in the process of neurodegeneration[4]; *WWC*, a gene associated with human memory performance[5]; *FEZ1* (MIM 604825), observed to be involved in axonal outgrowth[6]; *NPRL3* (MIM 600928), a regulator of mTOR signaling and associated with focal epilepsy and

cortical dysplasia (MIM 617118)[7; 8]; and *CUL4A* (MIM 603137), is involved in cell cycle progression and early embryogenesis[9; 10].

Supplemental Methods

SNP array, whole exome sequencing and whole genome sequencing

For Family 1, SNP genotyping was performed on genomic DNA from the proband and parents as previously described [11]; regions of homozygosity greater than 5Mb were selected for further analysis. Exome sequencing was performed using the Agilent SureSelect Target Enrichment Kit and the Illumina Hiseq 2000/2500 sequencer (Illumina, San Diego, CA) according to the manufacturer's instructions. Reads were aligned with human reference genome (hg19; NCBI build 37; Feb. 2009) using the Burrows-Wheeler Alignment Tool [12]. Variant calling was performed with GATK [13] and functionally annotated using SnpEff [14]. Because of consanguinity in the pedigree, homozygous variants were filtered based on allele frequencies less than 0.01 with no reported healthy homozygotes in online databases, dbSNP, 1000G, ESP6500 and ExAC. Likely pathogenicity was determined by online prediction tools (Polyphen, SIFT, CADD, and Mutation Taster) or if the variants were truncating (splicing or non-sense). For confirmation and family screening, the identified candidates were PCR amplified using primers flanking specific regions. PCR products were treated with BigDye V3.1 Terminator chemistry (Applied Biosystems, Warrington, UK) and electrophoresed on a ABI 3130xl genetic analyzer (Applied Biosystems, Foster city, CA, USA). The Sanger sequencing data were analyzed using Sequencher software (Gene Codes Corporation, Ann Arbor, MI, USA).

For Family 2, blood was collected in EDTA vials and DNA was extracted from all family members and subjected to genotyping (Axiom SNP chip platform) as described[15]. Index DNA was subjected to exome sequence by using TruSeq Exome Enrichment kit (Illumina) under the manufacturer's guidelines. Prepared sequence libraries were enriched using the Illumina Exome Enrichment protocol and sequenced using an Illumina HiSeq 2000 Sequencer. Sequenced reads were aligned against UCSC hg19 by BWA (see URL's). Homozygous variants (coding and splicing) within the 2MB region of ROH were considered as candidates based on the following criteria: MAF <0.01 in variant databases (see URL's) including 1000 Genomes, ExAC, gnomAD and exome variant server and in 2,379 in-house exomes; scores in SIFT, Polyphen and CADD Phred; and confirmation of identified homozygous variants by segregation in the family.

For Family 3, Whole Genome Sequencing was performed using the Illumina HiSeq sequencing platform. Briefly, DNA was extracted from the provided sample and measured for integrity via gel electrophoresis and appropriate concentration via fluorescent concentration determination. The DNA was then sonicated to a specific fragment size and prepared as a paired-end library with ligation of Illumina-flow cell specific adapter sequences and a unique barcode. Prepared library was then quality checked for adequate yield through fluorescent methods and quantitative PCR, as well as accurate library size and profile using bioanalysis. Libraries were clustered onto

Illumina HiSeq flow cells and sequenced using standard Illumina reagents and protocols. After sequencing, reads were generated using Illumina's bcl2 fastq and data were aligned to the human reference GRCh37. Using this technology, it is only possible to sequence 90% to 95% of the human reference genome. Analysis of the sequencing depth of all coding regions of the genome is available upon request. A gene with insufficient coverage may harbor variants that are not detected by this test. A gene may appear to have inadequate coverage when there is a deletion or insertion in the proband's gene sequence compared to the reference sequence.

For Family 4, exome sequencing was carried out on clinical basis. Genomic DNA was isolated from blood collected from proband and the parents by QIAamp DNA Blood Mini Kit (Qiagen, Valencia, CA, USA) according to manufacturer's instructions. Chromosomal microarray (CMA) was done on leukocyte-derived DNA of the proband using Illumina HumanCytoSNP-12. The genome-wide resolution of this array is ~30 kb. CMA showed no pathogenic copy number variants. A benign hemizygous deletion of size 296 kb was found at cytoband Xq28 (genomic coordinates 154939018-155235833 GRCh37/hg19) (genes SPRY3, VAMP7, IL9R), in addition to 19 regions of homozygosity. For exome sequencing, genomic capture was performed using Illumina's Nextera Rapid Capture Exome Kit. NextSeq500 Sequencer (Illumina, Inc., San Diego, CA, USA.) in combination with the NextSeq™ 500 High Output Kit (2×150 bp) was used for massive parallel sequencing. The raw data analysis and variant calling were performed based on GATK Best Practices for germline SNPs and Indels (version 3.6-0-g89b7209). Annotation of the called variants was done by ANNOVAR v.2016Feb01. Along with annotation, Online Mendelian Inheritance in Man (OMIM) and Human Phenotype Ontology (HPO) phenotypic information were also integrated using the in-house developed scripts. The strategy used for the variant filtering is as described in the Table S3. Candidate variants were validated and segregation analysis was carried out by Sanger sequencing.

For Family 5, genomic DNA was extracted from EDTA blood of the proband, her sister and her parents. Affymetrix Cytoscan (2.65 M) Array on the proband was performed calling bigger CNVs and regions of homozygosity greater than 3 Mb. Whole Exome Sequencing (WES) on the proband was performed using the Agilent SureSelectXT Kit (V6) with paired-end sequencing (HiSeq SBS Kit v4, 125 Fwd-125 Rev, Q30-value: 79.5) on a HiSeq System (Illumina Inc.). Raw fastQ files were aligned to the hg19 reference genome using NextGene (Softgenetics). Variants observed in at least 16% of reads with sufficient quality level and with Minor Allele Frequency ≤ 2% were investigated for deleterious In-Silico effects, by associations of the affected genes with proband's phenotype, by literature search for evident functional information and because of suspicion for consanguinity of the parents for homozygosity. The *TMEM94* (NM_014738.5) variants from the WES were confirmed in index, her sister and their patents after PCR amplification by Sanger sequencing using an ABI Genetic Analyzer 3730 (Applied Biosystems, Foster City, California).

For Family 6, clinical whole exome sequencing (XomeDx) was performed on the proband, mother, father and unaffected sister, at GeneDx (Gaithersburg, MD, USA).

Cell cycle assay

Skin derived fibroblasts from the affected individual from family 3 (Family 3-II.1) and two unaffected controls (purchased from ATCC, Manassas, VA, USA, catalogue number PCS-201-012) were seeded in 50-60% confluence. Cells were synchronized either by starvation in serum-free EBSS media for 48 hours, or treatment with 100ng/mL nocodazole overnight. Cells were then washed twice in cold phosphate buffered saline, and trypsinized. Harvested cells were subsequently fixed and stained with propidium iodide (PI) (NuCyclTM PI Kit; Exalpha Biologicals, Shirley, MA, USA) according to the manufacturer's instructions, and PI staining was quantified with a BD FACS Calibur flow cytometer (BD Biosciences, San Jose, CA, USA). The percentage of the cells in G0/G1, S, and G2/M phase were automatically counted and compared (FlowJo software; TreeStar, Ashland, OR, USA). The experiments were repeated in triplicate.

Supplemental References

1. Peretti, D., Bastide, A., Radford, H., Verity, N., Molloy, C., Martin, M.G., Moreno, J.A., Steinert, J.R., Smith, T., Dinsdale, D., et al. (2015). RBM3 mediates structural plasticity and protective effects of cooling in neurodegeneration. Nature 518, 236-239.
2. Zhu, X., Zelmer, A., Kapfhammer, J.P., and Wellmann, S. (2016). Cold-inducible RBM3 inhibits PERK phosphorylation through cooperation with NF90 to protect cells from endoplasmic reticulum stress. FASEB journal : official publication of the Federation of American Societies for Experimental Biology 30, 624-634.
3. Li, Y.S., Milner, P.G., Chauhan, A.K., Watson, M.A., Hoffman, R.M., Kodner, C.M., Milbrandt, J., and Deuel, T.F. (1990). Cloning and expression of a developmentally regulated protein that induces mitogenic and neurite outgrowth activity. Science 250, 1690-1694.
4. Wetzel, M.K., Naska, S., Laliberte, C.L., Rymar, V.V., Fujitani, M., Biernaskie, J.A., Cole, C.J., Lerch, J.P., Spring, S., Wang, S.H., et al. (2008). p73 regulates neurodegeneration and phospho-tau accumulation during aging and Alzheimer's disease. Neuron 59, 708-721.
5. Papassotiropoulos, A., Stephan, D.A., Huentelman, M.J., Hoerndli, F.J., Craig, D.W., Pearson, J.V., Huynh, K.D., Brunner, F., Corneveaux, J., Osborne, D., et al. (2006). Common Kibra alleles are associated with human memory performance. Science 314, 475-478.
6. Bloom, L., and Horvitz, H.R. (1997). The Caenorhabditis elegans gene unc-76 and its human homologs define a new gene family involved in axonal outgrowth and fasciculation. Proc Natl Acad Sci U S A 94, 3414-3419.
7. Ricos, M.G., Hodgson, B.L., Pippucci, T., Saidin, A., Ong, Y.S., Heron, S.E., Licchetta, L., Bisulli, F., Bayly, M.A., Hughes, J., et al. (2016). Mutations in the mammalian target of rapamycin pathway regulators NPRL2 and NPRL3 cause focal epilepsy. Annals of neurology 79, 120-131.
8. Sim, J.C., Scerri, T., Fanjul-Fernandez, M., Riseley, J.R., Gillies, G., Pope, K., van Roozendaal, H., Heng, J.I., Mandelstam, S.A., McGillivray, G., et al. (2016). Familial cortical dysplasia caused by mutation in the mammalian target of rapamycin regulator NPRL3. Annals of neurology 79, 132-137.
9. Kopanja, D., Stoyanova, T., Okur, M.N., Huang, E., Bagchi, S., and Raychaudhuri, P. (2009). Proliferation defects and genome instability in cells lacking Cul4A. Oncogene 28, 2456-2465.
10. Li, B., Ruiz, J.C., and Chun, K.T. (2002). CUL-4A is critical for early embryonic development. Molecular and cellular biology 22, 4997-5005.
11. Stephen, J., Vilboux, T., Haberman, Y., Pri-Chen, H., Pode-Shakked, B., Mazaheri, S., Marek-Yagel, D., Barel, O., Di Segni, A., Eyal, E., et al. (2016). Congenital protein losing enteropathy: an inborn error of lipid metabolism due to DGAT1 mutations. European journal of human genetics : EJHG 24, 1268-1273.
12. Li, H., and Durbin, R. (2009). Fast and accurate short read alignment with Burrows-Wheeler transform. Bioinformatics (Oxford, England) 25, 1754-1760.

13. McKenna, A., Hanna, M., Banks, E., Sivachenko, A., Cibulskis, K., Kernytsky, A., Garimella, K., Altshuler, D., Gabriel, S., Daly, M., et al. (2010). The Genome Analysis Toolkit: a MapReduce framework for analyzing next-generation DNA sequencing data. Genome research 20, 1297-1303.
14. Cingolani, P., Platts, A., Wang le, L., Coon, M., Nguyen, T., Wang, L., Land, S.J., Lu, X., and Ruden, D.M. (2012). A program for annotating and predicting the effects of single nucleotide polymorphisms, SnpEff: SNPs in the genome of Drosophila melanogaster strain w1118; iso-2; iso-3. Fly 6, 80-92.
15. Alkuraya, F.S. (2012). Discovery of rare homozygous mutations from studies of consanguineous pedigrees. Current protocols in human genetics Chapter 6, Unit6.12.